Volume 1 | Number 1 | Jan 2013 | Pages 1–100

Soft Matter

www.rsc.org/softmatter

ROYAL SOCIETY OF CHEMISTRY

ROYAL SOCIETY OF CHEMISTRY

www.rsc.org/softmatter

Modeling the effect of surface forces on the equilibrium liquid profile of a capillary meniscus

**Igor V. Kuchin[1], Omar K. Matar[2], Richard V. Craster[3], Victor M. Starov[1*]**

[1]Department of Chemical Engineering, Loughborough University, Loughborough, LE113TU, UK

[2]Department of Chemical Engineering, Imperial College London, South Kensington Campus, London SW72AZ, UK

[3]Department of Mathematics, Imperial College London, South Kensington Campus, London SW72AZ, UK

Table of contents entry

Effect of the surface forces action on equilibrium profile of a meniscus in a vicinity of an apparent three phase contact line under a combined action of disjoining/conjoining and capillary pressures is modelled and analysed.
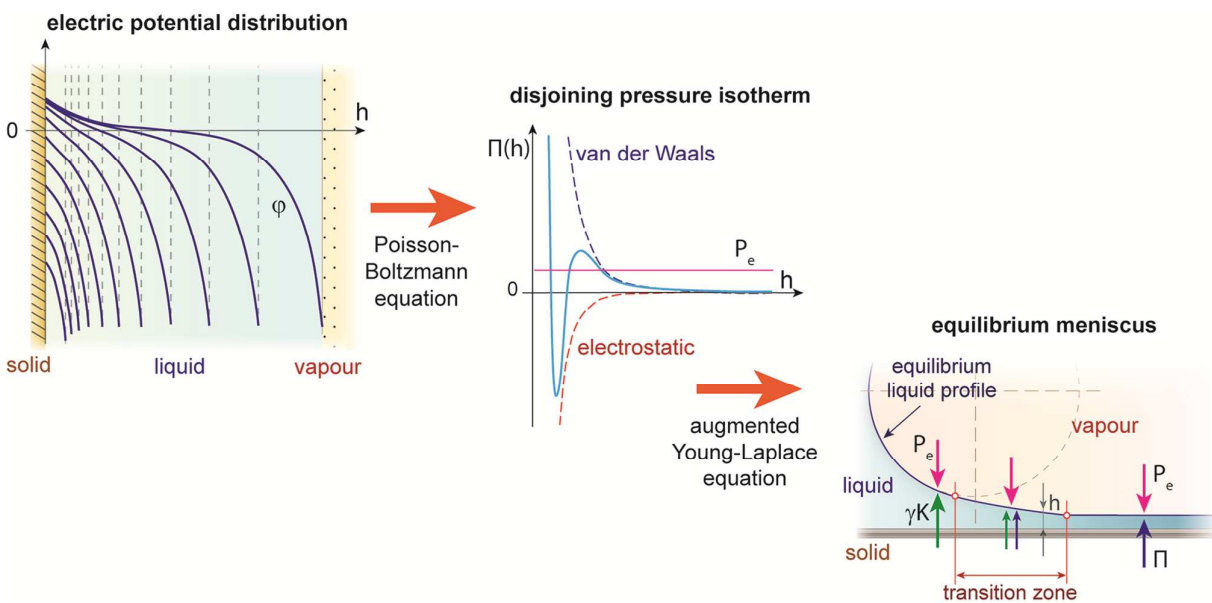
Abstract

Equilibrium profile of a capillary meniscus formed under combined action of disjoining/conjoining and capillarity pressures is investigated. Attention is focused on the shape of a transition zone between a spherical meniscus and a thin liquid film in front of the meniscus. Poisson-Boltzmann equation is used for calculations of electrostatic contribution to the disjoining/conjoining pressure and the liquid shape inside the transition zone. Both complete and partial wetting conditions are investigated.

Keywords: disjoining/conjoining pressure, double electric layer, Poisson-Boltzmann equation.

*Corresponding author: V.M.Starov@lboro.ac.uk

1

1. Introduction

Disjoining/conjoining pressure is a manifestation of surface forces acting in thin liquid layers. This concept was introduced and successfully investigated in the pioneering works of Derjaguin.[1,2] Since then this concept has had widespread applications in interactions in colloid systems, such as suspensions, emulsions, foams, liquid films on solid surfaces. The well-known DLVO theory of colloidal stability is completely based on the disjoining/conjoining pressure acting between colloidal objects (for example, particles/droplets).[1] Disjoining/conjoining pressure also acts in a vicinity of a three-phase contact line in the case of wetting/spreading.[3] However, for historical reasons the action of disjoining/conjoining pressure action in the case of wetting/spreading has received less attention. Still there is a number of publications where the effect of surface forces on wetting and spreading phenomena of liquids on solid substrates is considered (see[4-7] and references therein).

Liquid wetting films on solid substrates exist because the disjoining/conjoining pressure inside the liquid film is balanced by the capillary pressure in the neighbouring meniscus or droplet. Inside spherical part of a meniscus or a droplet the separation between the liquid-vapour and solid-liquid interfaces is bigger than radius of the disjoining/conjoining pressure action. Hence, the shape of the meniscus or droplet is determined by the action of capillary pressure only.[3] Hence, a transition zone must exist in between a droplet/meniscus and a flat thin liquid film in front where the disjoining/conjoining pressure and capillary pressure act simultaneously.[3,5,7] The size and shape of the transition zone is essential because experimental measurements of equilibrium/hysteresis contact angles and surface curvature of bulk liquids are carried out outside this transition zone. It is well known that disjoining/conjoining pressure cannot be measured in the whole range of surface forces action[1], hence, the shape of liquid inside the transition zone may supply information on the disjoining/conjoining pressure isotherm in the range where direct experimental measurements of disjoining/conjoining pressure are currently impossible.

Below we model equilibrium liquid profiles inside the transition zone between a capillary meniscus and a thin liquid film in front. A low-slope approximation for the liquid interface in the transition zone is used which allows using isotherm of disjoining/conjoining pressure of flat liquid films.[1,8-9] Equilibrium conditions in both normal and tangential directions are satisfied using this approach. Disjoining/conjoining pressure isotherms are obtained by direct solution of Poisson-Boltzmann equation with appropriate boundary conditions. This enables us analysing the

2

electrostatic component of disjoining/conjoining pressure and its dependence on properties of the system under investigation. The effect of disjoining/conjoining pressure is discussed for both complete and partial wetting conditions.

2. Disjoining/conjoining pressure and wetting phenomena

2.1. Equilibrium flat wetting films

Let us consider the conditions of equilibrium for flat wetting films in contact with a liquid meniscus or a droplet.

Kelvin's equation describes the change in vapour pressure over the curved liquid/vapor interface (for example, a capillary or a droplet)[20]:

$$P_e = \frac{RT}{v_m}\ln\frac{p_s}{p}$$
                                                                                                (1)

where $P_e = P_a - P_l$ is the excess pressure; P_l is the pressure inside the liquid; P_a is the pressure in the ambient vapour; v_m is the liquid molar volume; p_s and p are the saturated vapour pressure and the pressure over the curved interface, respectively; p_s is the equilibrium vapour pressure over a flat liquid surface. The excess pressure inside the droplet, P_e, should be negative (pressure inside the droplet is higher than the pressure in the ambient vapour). Thus, the right-hand side of Kelvin's equation must be negative, which is possible only if $p > p_s$; that is, droplets can only be at equilibrium with oversaturated vapour. It is difficult to investigate experimentally equilibrium droplets on solid substrates because it is necessary to maintain oversaturated vapour over the substrate under investigation for a prolonged period of time[3].

In contrast to a droplet equilibrium for a meniscus according to the Kelvin's equation is possible with undersaturated vapour ($P_e > 0$ and $p < p_s$). Note, equilibrium meniscus can exist in the case of both complete and partial wetting. The latter is different from equilibrium droplets, which can exist only in the partial wetting case; in the case of complete wetting droplets spread out completely. In this section we focus on the transition zone of a meniscus in the case of complete wetting.

In Fig. 1 a schematic presentation of two possible shapes of disjoining/conjoining pressure isotherms is given. These types of dependence, $\Pi(h)$, are typical for the sum of electrostatic and van der Waals components of the disjoining/conjoining pressure (DLVO theory). Dependency 1 in Fig. 1 corresponds to the complete wetting case, while curve 2 usually corresponds to the partial wetting case.

The thickness h_e of the equilibrium wetting film in this case corresponds to the intersection of a straight line $P_e > 0$ with the disjoining/conjoining pressure isotherm: there is a only one intersection in the case 1 in Fig. 1, which corresponds to the complete wetting case.

It could be three intersections of a straight line $P_e > 0$ (isotherm 2 in Fig.1) with the disjoining/conjoining pressure isotherm. However, h_β and h_u are a metastable and an unstable equilibrium thicknesse, respectively; only h_e corresponds to a thermodynamically stable equilibrium thickness.[1,3]
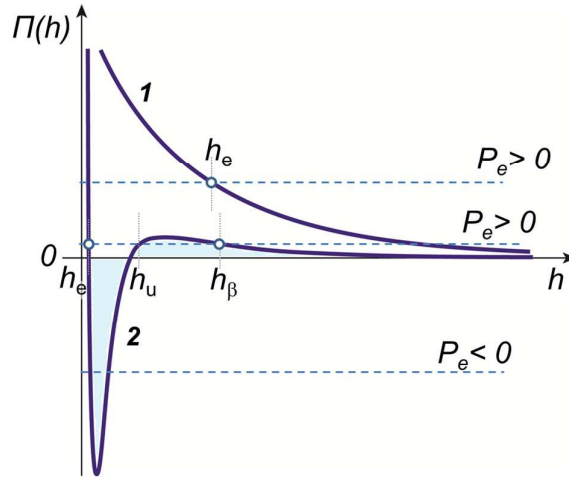
Fig. 1. Schematic presentation of disjoining/conjoining pressure isotherms.

(1) complete wetting case, (2) partial wetting case.

h_e, h_u, h_β – thicknesses of a stable, an unstable and a metastable wetting films respectively.[1,3]

The shape of the isotherms is typical for a sum of electrostatic and van der Waals interactions

(DLVO theory).

The equilibrium contact angle in terms of disjoining/conjoining pressure is determined[1,3] as

$$\cos \theta_e = 1 + \frac{1}{\gamma} \int_{h_e}^{\infty} \Pi(h) dh$$

(2)

where Π is disjoining pressure; γ is the liquid-vapour interfacial tension.

There are two possible situations in geometrical definition of equilibrium contact angle θ_e:

(i) $H < r_e$ (Fig. 2, case 2), this situation is referred to as partial wetting case and contact angle is defined as $\cos \theta_e = H/r_e < 1$;

(ii) $H > r_e$ (Fig. 2, case 1), this situation is referred to as complete wetting; the contact angle cannot be introduced geometrically. The case of complete wetting is characterised below by the ratio H/r_e which can be referred to as '$\cos \theta_e > 1$'.
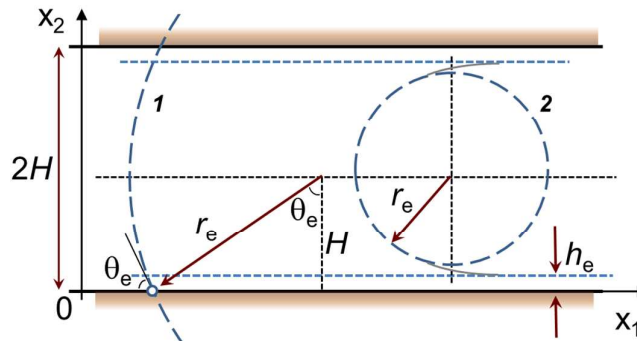
Fig. 2. A schematic presentation of two possible positions of a spherical meniscus inside a two dimensional capillary.

(*1*) partial wetting, $r_e > H$, $\cos \theta_e = H/r_e < 1$;

(*2*) complete wetting, $r_e < H$, $H/r_e > 1$.

For the complete wetting case the integral in the right-hand side in Eq.(2) is always positive[3,11] (see curve 1 in Fig.1). For partial wetting conditions ($\cos \theta_e < 1$), the integral inh the right hand site of Eq. (2) of the disjoining/conjoining pressure is negative (Fig.1, curve 2).

A statistical mechanics approach to the disjoining/conjoining pressure of planar films in application to wetting phenomena was presented in[21-22].

2.2. Equation for equilibrium liquid profile

The excess free energy should reach its minimum value for any equilibrium liquid profile $h(x)$. The following requirements must be satisfied for this to occur: (i) the first variation of the excess Gibbs free energy, δG, vanishes, (ii) the second variation, $\delta^2 G$, is positive, and (iii) the transversality condition at the three-phase contact line should be satisfied.[3] The excess Gibbs free energy, G, of a non-flat liquid layer, for example, a droplet or a meniscus on a solid substrate is expressed in the absence of gravity[3,10] as:

$$G = \gamma S + P_e V + G_D - G_{ref},\tag{3}$$

where S, V, and G_D are the excess vapour-liquid interfacial area, the excess volume, and the excess energy associated with the surface forces action, respectively; G_{ref} is the excess free energy of a reference state, which is the excess free energy of an equilibrium flat liquid film of thickness h_e.

Below for simplicity only two dimensional equilibrium systems are under investigation. In this case the excess free energy (3) can be rewritten as:

$$G = \int \left\{ \gamma \left(\sqrt{1 + h'^2} - 1 \right) + P_e(h - h_e) + \int_h^\infty \Pi_e(h)dh - \int_{h_e}^\infty \Pi_e(h)dh \right\} dx_1 ,$$ (4)

where ' denotes differentiation with respect to a coordinate x_1 along the profile. The equilibrium liquid profile corresponds to the minimum of the excess free energy (4), which can be obtained using the Euler equation:

$$\frac{\partial f}{\partial h} - \frac{d}{dx_1} \frac{\partial f}{\partial h'} = 0$$ (5)

where $f = \gamma \left(\sqrt{1 + h'^2} - 1 \right) + P_e(h - h_e) + \int_h^\infty \Pi_e(h)dh - \int_{h_e}^\infty \Pi_e(h)dh$ is the integrand in Eq. (4). This results in the following augmented Young-Laplace equation:

$$P_e - \Pi_e(h) - \frac{d}{dx_1} \frac{\gamma h'}{\sqrt{1 + (h')^2}} = 0$$ (6)

In the case of a constant surface tension and in the low-slope approximation, $(h')^2 \ll 1$, Eq. (6) takes the following form:

$$\gamma h'' + \Pi_e(h) = P_e$$ (7)

The subscript e in Π_e corresponds to the state of equilibrium between the capillary and disjoining/conjoining pressures as described by Eq.(7). This is the equation for equilibrium meniscus profile satisfying the condition of the minimum of the excess free energy G in the low-slope approximation.

3. Model description

3.1. Model assumptions

Let us consider an equilibrium transition zone *II* (Fig. 3) between a two dimensional capillary meniscus (*I*) and a flat wetting film (*II*). We use a rectangular coordinate system, (x_1, x_2), where x_1, x_2 are the tangential and normal coordinates, respectively. The width of the capillary, *2H,* is assumed to be much larger than the thickness of the equilibrium flat film, h_e. In the case under consideration, the thickness of the liquid layer, $h(x_1)$, is a function of x_1 only, as shown in Fig. 3, where the meniscus in the case of complete wetting is sketched: a continuation of a spherical meniscus (broken line) of radius r_e does not intersect either the solid walls of the capillary or the thin liquid film of thickness h_e. The partial wetting case is considered below in the next section.
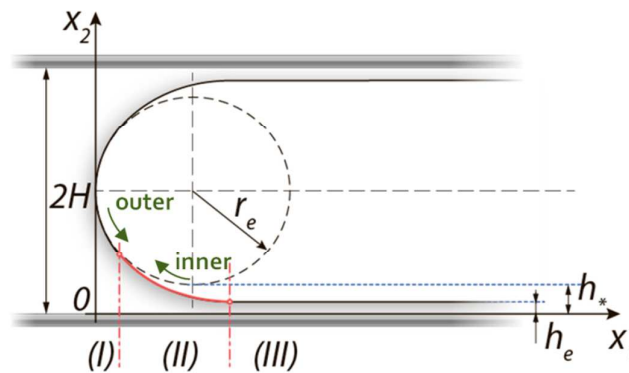
Fig. 3. A schematic presentation of a capillary meniscus in the case of complete wetting. The regions *I*, *II*, and *III* correspond to the spherical capillary meniscus, the transition zone and the flat equilibrium film, respectively. The radius of curvature of the meniscus, r_e, is smaller than the half width *H*. The values r_e and h_e are to be determined below.

An aqueous solution of a binary univalent symmetric strong electrolyte is considered below. All surface forces additional to the capillary forces are supposed to be caused by electrostatic interaction between the charged surfaces only. All other surface forces (including van der Waals forces) are neglected on this stage. There is no flow under equilibrium conditions and all ion fluxes vanish. The surface tension is assumed constant, which is valid in the absence of surfactants.[12,13]

3.2. Governing equations

The expression for electrostatic component of disjoining/conjoining pressure was derived for the case of low-slope interface profile (see Appendix 1):

$$\Pi(h) = RTc_0 \left(\exp(\varphi) + \exp(-\varphi) \right) \Big|_{x_2=h} - \frac{(RT)^2 \varepsilon \varepsilon_0}{2F^2} \left(\frac{\partial \varphi}{\partial x_2} \right)^2_{x_2=h} - 2RTc_0 \tag{8}$$

where $\varphi = \Phi F/(RT)$ is a dimensionless potential in which the dimensional potential, Φ, is made dimensionless using F/RT, where F is the Faraday constant, R is the gas constant, and T is the absolute temperature, respectively; c_0 is the molar electrolyte concentration; ε and ε_0 are the dielectric constants of water and vacuum, respectively.

Eq. (8) was obtained using Poisson-Boltzmann equation in combination of the condition of normal-stress balance for the interface profile (see Appendix 1 for details). Eq.(8) coincides with wel-known expression for electrostatic component of disjoining pressure obtained for flat films[1,16]. Derivation presented in Appendix 1 shows that it is also valid for the case of non-flat thin liquid layers in the case of low-slope approximation.

Calculation of the dependence $\Pi(h)$ according to Eq.(8) requires the knowledge of two functions, $\varphi(h)$ and $\varphi'(h)$, at the liquid-vapour interface, $x_2 = h$. These functions can be determined by numerical integration of Poisson-Boltzmann equation:

$$\frac{\partial^2 \varphi}{\partial x_2^2} = \frac{F^2 c_0}{RT\varepsilon\varepsilon_0}(\exp(\varphi) - \exp(-\varphi)).$$

(9)

The following boundary conditions are used below for integration of Poisson-Boltzmann Eq. (9) in order to calculate the electric potential distribution $\varphi(x_2)$ and $\partial\varphi/\partial x_2$ across the liquid film:

a) constant surface electrical potentials on both liquid-solid and liquid-vapour interfaces: φ_s, φ_h = const;

b) constant surface charge densities σ_s, σ_h = const.

These two case are selected because according to Derjaguin *et al.*[1] the cases φ= constant and σ= constant are the limiting cases for all possible boundary conditions: the minimum possible values of disjoining/conjoining pressure corresponds to the case φ= const, whereas the σ constant case corresponds to the maximum values of disjoining/conjoining pressure. All other physically possible situations for both an electric potential and surface charge variation on the boundaries results in disjoining/conjoining pressure isotherms located in between curves 1 and 2 (see below Fig. 7).

Conditions φ_s, φ_h = const or σ_s, σ_h = const mean that at variation of the thickness, h, the boundary values of potential φ or surface charge σ remain constant on both boundaries of the film (but variable inside the film). The situations when $\varphi_s \neq \varphi_h$ or $\sigma_s \neq \sigma_h$ are rather common.

The equilibrium interfacial profile under the action of the surface forces is described by the augmented Young-Laplace equation (6) or (7) originally proposed by Derjaguin[1]:.

Eq.(7) or (A14) in Appendix 1 are the particular cases of (6) for the low-slope interface ($h'^2 \ll 1$); these equations are solved using the following boundary conditions:

$$x_1 \to \infty, h = h_e, \ h' = 0 \tag{10}$$

The unknown values of the radius of the equilibrium meniscus, r_e, and the thickness of the equilibrium flat film, h_e, are determined below before calculating the equilibrium profile. The latter is determined using a procedure of matching the inner and outer asymptotic solutions (see Appendix 2).

Eq. (6) for the flat film ($h = h_e$; $h', h'' = 0$) in combination with Eq. (8), solved simultaneously with Eq. (A17) gives a system of two equations for two unknown values h_e and $h^* = H - r_e$:

8

$$\begin{cases} \Pi_e(h_e) = RTc_0\big(exp(\varphi) + exp(-\varphi)\big)_{x_2=h_e} - \frac{(RT)^2 \varepsilon\varepsilon_0}{2F^2}\left(\frac{\partial \varphi}{\partial x_2}\right)^2_{x_2=h_e} - 2RTc_0 = \frac{\gamma}{H - h_*} \\ h_* = h_e + \frac{H - h^*}{\gamma}\int_{h_e}^{\infty} \Pi_e(h)dh \end{cases}$$

$$(11)$$

The values h_e and h^* determined from Eqs. (11) allow calculating equilibrium meniscus profile inside the transition zone using Eq. (7).

4. Results and discussion

In this section distribution of electric potential is determined using boundary conditions of constant potential or constant charge. After that dependences of the disjoining/conjoining pressure and the shape of the interface are deduced. An aqueous solution of univalent strong electrolyte NaCl is used at temperature $T = 293$ [K]; bulk NaCl concentration $c_0 = 1$ and 1×10^3 [mole/m³]; surface tension of solution $\gamma = 72.7$ and 74.7×10^{-3} [N/m], respectively; the width of the capillary $H = 3\times10^{-6}$ and 3×10^{-7}, [m]. The well-known expressions[1,16] relating σ and φ on the boundaries are used:

$$\sigma_h = \varepsilon\varepsilon_0 \frac{RT}{F}\left(\frac{\partial \varphi}{\partial x_2}\right)_{x_2=h} \quad \text{for the liquid/vapour interface;}$$

$$\sigma_s = -\varepsilon\varepsilon_0 \frac{RT}{F}\left(\frac{\partial \varphi}{\partial x_2}\right)_{x_2=0} \quad \text{for the solid/liquid interface} \qquad (12)$$

The Poisson-Boltzmann equation was solved for various values of separation h with the fixed boundary values of surface potentials or surface charges. Two cases are considered below: (i) symmetric potential profiles for electrically similar surfaces having the identical boundary values of either electric potentials or charges, that is, $\varphi_s = \varphi_h$ or $\sigma_s = \sigma_h$; (ii) asymmetric profiles for electrically dissimilar surfaces having different boundary values of electric potentials or charges, that is, $\varphi_s \neq \varphi_h$ or $\sigma_s \neq \sigma_h$.

4.1. Electrically similar surfaces

For the case $\varphi_{h,s} = $ const, the electric potential φ changes inside the liquid, but the boundary values of φ are fixed. The constancy of the boundary potentials $\varphi_{h,s}$ is achieved at the expense of a change in the surface charges, $\sigma_{h,s}$ (see Fig. 4a). This change corresponds to variation of the slope of the curves $\varphi(h)$ at both surfaces, as can be seen from Eq. (12). This variation in the charge corresponds to a redistribution of ions between the liquid phase and the surfaces due to adsorption/desorption.

In this section symmetric boundary conditions $\varphi_s = \varphi_h$ were selected. As a result, the surface charges are also symmetric: $\sigma_s = \sigma_h$. In this case (see Fig. 4b) the disjoining/conjoining pressure is positive, $\Pi(h) > 0$, which corresponds to repulsion between the interfaces: this is the consequence of identical charges of both liquid-air and solid-liquid interfaces: $\sigma_s = \sigma_h$.

In the case of $\sigma_{h,s} = $ constant two situations are considered below: the interacting surfaces are similarly charged, or oppositely charged. In the first case repulsion between the surfaces is expected, whilst in the second case attraction may take place.

The results are presented in Fig. 5 (for the case of similarly charged surfaces, $\sigma_s > 0$, $\sigma_h > 0$) and in Fig. 6 (for the case of oppositely charged surfaces, $\sigma_s > 0$, $\sigma_h < 0$). In the case of identically charged surfaces, the identical values of surface potentials were obtained, that is, $\varphi_s = \varphi_h$ (see Fig. 5a). However, in the case of oppositely charged surfaces potentials φ_s and φ_h vary in a different way (Fig. 6a): similarly to the charges they are of opposite sign, $\varphi_s = -\varphi_h$. As a result in the case of identical charges of both interfaces, the repulsion is obtained, $\Pi(h) > 0$ (Fig. 5b); while in the case of oppositely charged interfaces, it results in attraction, $\Pi(h) < 0$ (Fig. 6b). However, Fig. 6b shows that in the second case $d\Pi/dh < 0$, so any flat wetting films for this cased are unstable and flat films cannot exist under these conditions.[3,4]
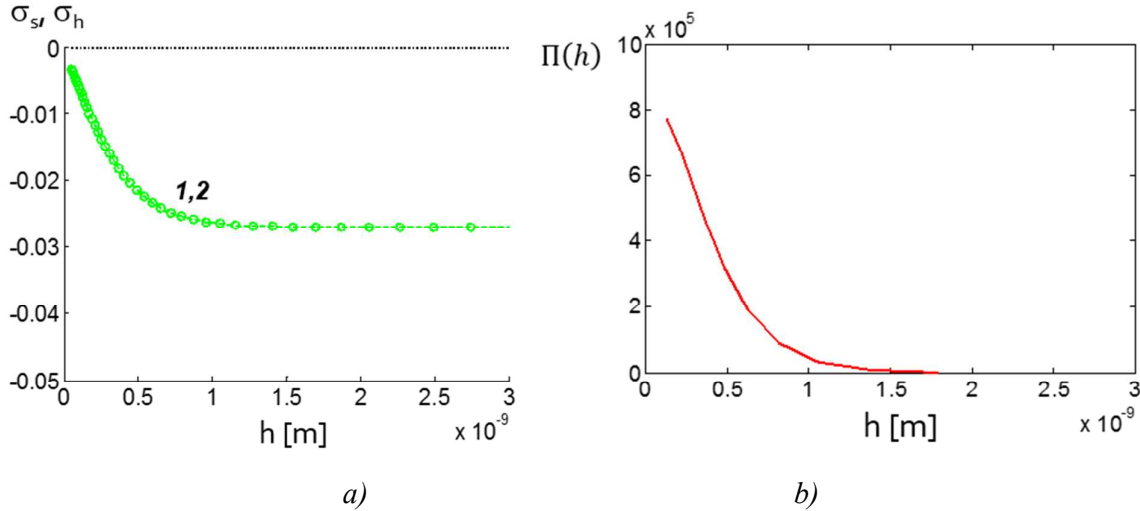
Fig. 4. Dependencies of the surface charge (a), according to Eq. (12); disjoining/conjoining pressure isotherm (b), according to Eq. (8). The case of constant surface potentials, $\varphi_{h,s} = $ constant. The parameter values are $\Phi_s = -15$ mV, $\varphi_s = -0.6$; $\Phi_h = -15$ mV, $\varphi_h = -0.6$. (a): 1 and 2 correspond to the solid/liquid (σ_s) and vapour/liquid (σ_h) interfaces, respectively.

a)   *b)*
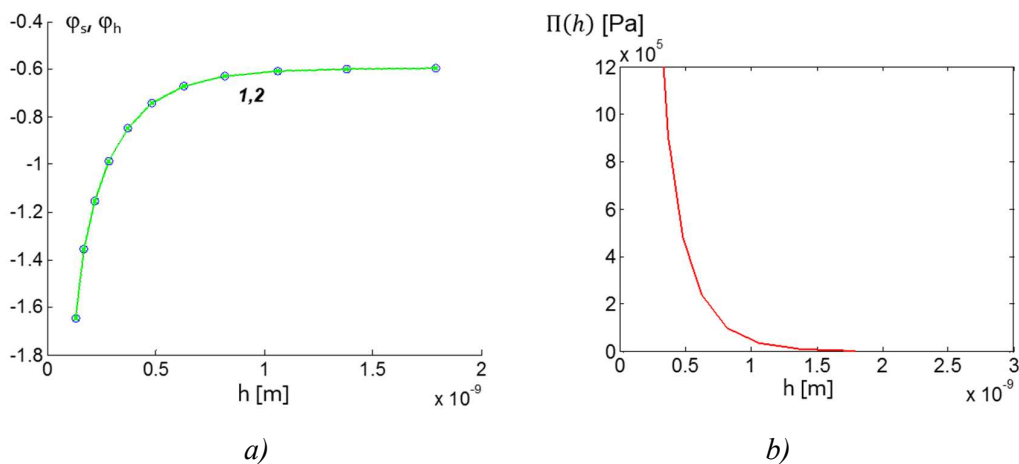
Fig. 5. Dependencies of the surface electric potentials (*a*); disjoining/conjoining pressure isotherm (*b*), according to Eq. (8). The case of constant surface charges, $\sigma_s > 0$, $\sigma_h > 0$, $\sigma_{h,s}$ = constant, $\sigma_s = 27$ 10^{-3} C, $\sigma_h = 27$ 10^{-3} C. (*a*): *1* and *2* correspond to the solid/liquid (φ_s) and vapour/liquid (φ_h) interfaces, respectively.

*a)*   *b)*
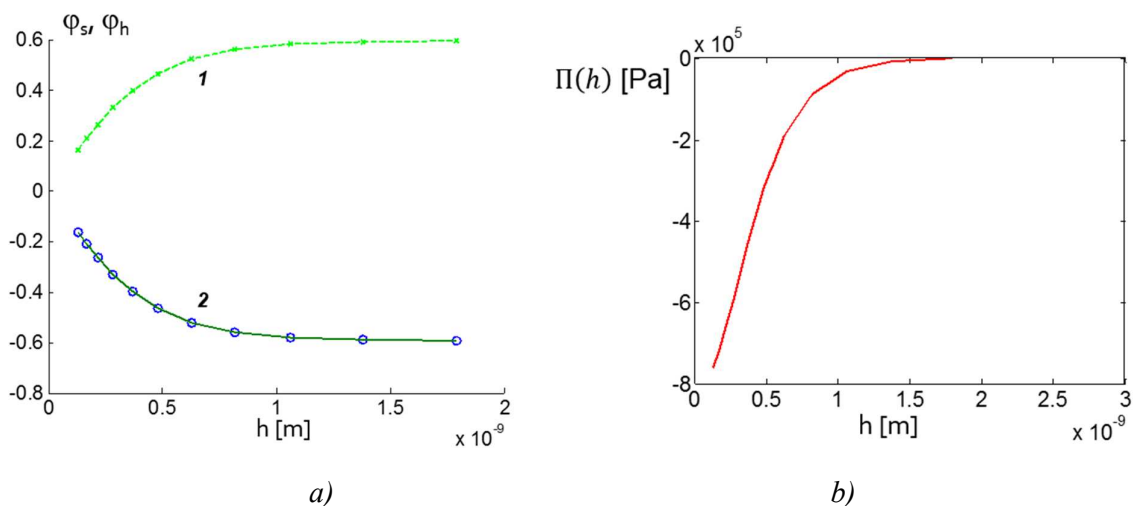
Fig. 6. Dependencies of the surface electric potentials (*a*); disjoining/conjoining pressure isotherm (*b*), according to Eq. (8). The case of constant surface charges, $\sigma_s > 0$, $\sigma_h < 0$; $\sigma_{h,s}$ = const, $\sigma_s = 27$ 10^{-3} C, $\sigma_h = -27$ 10^{-3} C. (*a*): *1* and *2* correspond to the solid/liquid (φ_s) and vapour/liquid (φ_h) interfaces, respectively.

It is important to compare the disjoining/conjoining pressure isotherms presented in Figs. 4 and 5. The dependencies have different character at small separations but coincide at large *h* (Fig. 7). The latter is because at large distances only slight overlapping of the electric double layers takes place. However, in the case of small separations the interaction is stronger and the difference in boundary conditions becomes important. In the case σ = constant the disjoining/conjoining pressure

diverges as $h \to 0$ (curve 2), whereas for φ = constant disjoining/conjoining pressure (curve 1) has y-axis intercept corresponding to the maximum possible value of $\Pi(h)$.

The disjoining/conjoining pressure isotherms calculated using Eq. (8) with two types of boundary conditions (Fig. 7) qualitatively agree with results of Derjaguin *et al.*[1] As already was mentioned above according to Derjaguin *et al.*[1] all other physically possible situations for both an electric potential and surface charge variation on the boundaries results in disjoining/conjoining pressure isotherms located in between curves 1 and 2 in Fig. 7.
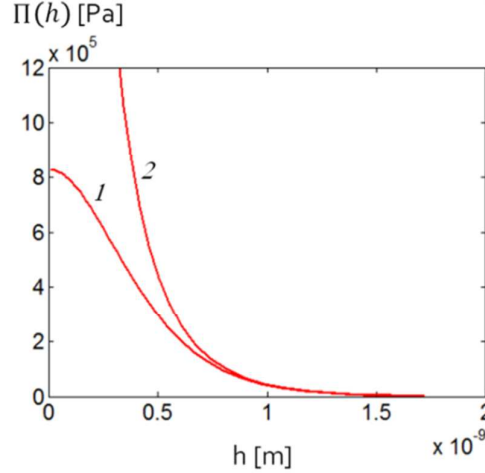
Fig. 7. Comparison of disjoining/conjoining pressure isotherms for different types of boundary conditions.

Calculation using Eq. (8): *1.* φ = const = -0.6 (Φ = -15 mV), *2.* σ= const = -27 mC.

4.2. Equilibrium flat liquid film

Equilibrium condition for flat liquid films corresponds to equality of disjoining/conjoining and capillary pressures inside meniscus/drop, the film is in contact with. This equality follows from Eq. (6) at $h', h'' = 0$:

$$RTc_0\left(\exp(\varphi)+\exp(-\varphi)\right)\Big|_{x_2=h} - \frac{(RT)\varepsilon\varepsilon_0}{2F^2}\left(\frac{\partial\varphi}{\partial x_2}\right)^2_{x_2=h} - 2RTc_0 = \frac{\gamma}{r_e}$$

Solution of the latter equation corresponds to points of intersection of the disjoining/conjoining pressure isotherm and the straight line, as shown in Fig. 8,*a*. This intersection is always possible in the case σ= constant. However, in the case φ = constant the high values of the capillary pressure ($\gamma/r_e > \Pi_{max}$) cannot be counterbalanced by the disjoining/conjoining pressure; such situation occurs in thin capillaries at $r_e < \gamma/\Pi_{max}$.

A maximum disjoining/conjoining pressure value Π_{max} is found below using the following consideration: the Maxwell part of the disjoining/conjoining pressure tends to zero at small separations (Fig. 8,*b*) at $\varphi_s = \varphi_h$ = constant: $\lim_{h \to 0} \frac{\partial \varphi}{\partial x_2} = 0$. Hence, the maximum value of the disjoining/conjoining pressure is equal to an excess osmotic pressure in the film as compared with the bulk phase:

$$\Pi_{max} = RTc_0\left(\exp(\varphi_h) + \exp(-\varphi_h)\right) - 2RTc_0 \tag{13}$$
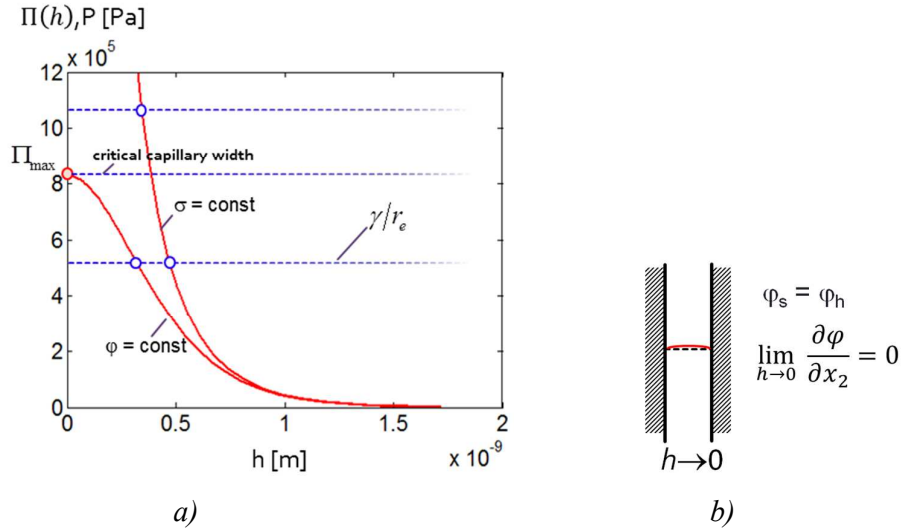
Fig. 8. Condition of equilibrium between disjoining/conjoining and capillary pressures (*a*); vanishing the Maxwell part of disjoining/conjoining pressure at small separations (*b*).

Equating right hand site of Eq. (13) and γ/r_e, and assuming that $\gamma/r_e \approx \gamma/H$, the critical capillary half width H^{cr} corresponding to the equality $\Pi_{max} = \gamma/H^{cr}$ can be obtained as:

$$H^{cr} = \frac{\gamma}{c_0 RT(\exp(\varphi_h) + \exp(-\varphi_h) - 2)} \tag{14}$$

The dependence H^{cr} on electric potential $\Phi_h = \varphi_h RT/F$ is shown in Fig. 9.
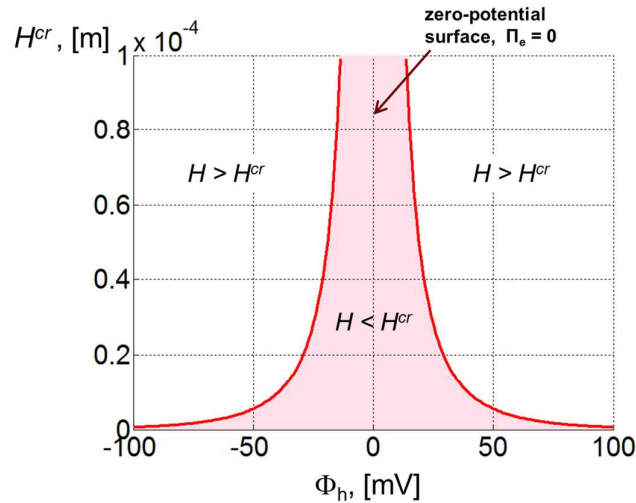
Fig. 9. The critical capillary half width H^{cr} as a function of the electric potential on the boundary $x_2 = h$

at $T = 293$ [K]; $c_0 = 1$ [mole/m^3]; $\gamma = 72.7 \times 10^{-3}$ [N/m]; $\varphi_{h,s} = $ const.

Fig. 9 shows that the equilibrium between the disjoining/conjoining and capillary pressures is possible only in the region $H > H^{cr}$, where the capillary pressure is less than Π_{max}. The region $H < H^{cr}$ between the two branches of the dependence $H^{cr}(\Phi_h)$ in Fig. 9 corresponds to thin capillaries and low potentials Φ_h. Inside this 'prohibited' zone the capillary pressure is too high or the disjoining/conjoining pressure is too low and, hence, equilibrium is impossible and flat films do not exist.

4.3. Interaction of electrically dissimilar surfaces

In the previous section the cases $\varphi_{h,s} = $ constant and $\sigma_{h,s} = $ constant with symmetric conditions on both boundaries were considered. It was assumed that the values of the electric charge or electric potential were identical on both solid-liquid and liquid-vapour interfaces. Now we consider films with electrically dissimilar interfaces for values of electric potential (or surface charge) that are different on both the vapour-liquid and liquid-solid interfaces. Note in this case the boundary values are different, but still fixed, i.e. they are supposed not to depend on the film thickness h.

a)

b)

c)
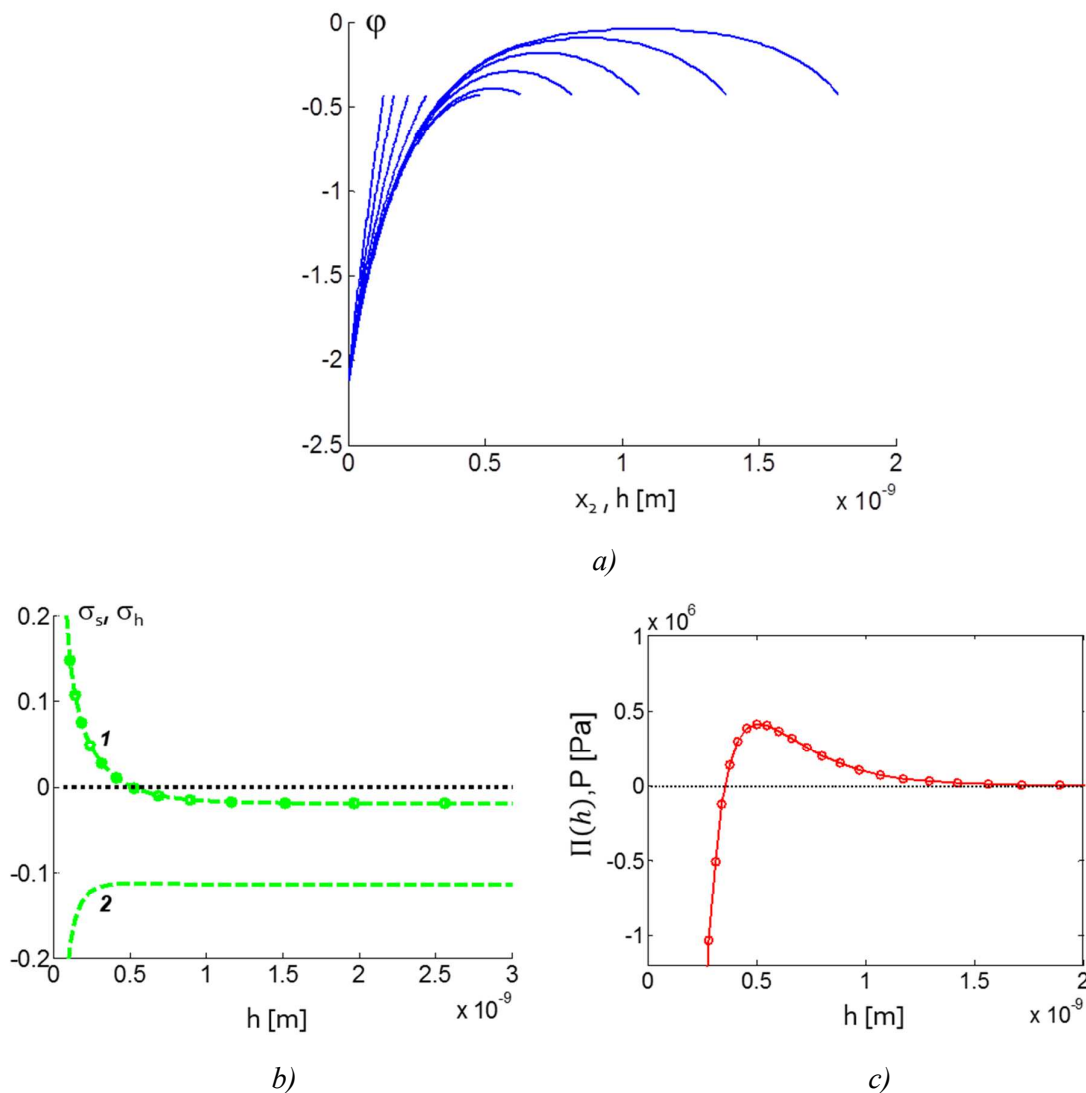
Fig. 10. Interaction of electrically dissimilar surfaces for the case of constant surface potentials, $\varphi_{h,s}$ = const. *a)* electric potential distribution, according to Eq. (9): φ_s = -2.12 (Φ_s = -53.5 mV), φ_h = -0.42 (Φ_h = -10.6 mV); *b)* surface charges $\sigma_{h,s}$ variation, according to Eq. (12): *1*- liquid/vapour interface, *2*- solid/liquid interface; *c)* disjoining/conjoining pressure isotherm according to Eq. (8).

In the case of constant but different electric potentials $\varphi_s \neq \varphi_h$, the calculations using the Poisson-Boltzmann Eq. (9) results in an asymmetric distribution of electric potentials (Fig. 10*a*). Since the boundary values of φ are fixed the surface charges $\sigma_{h,s}$ vary (see Fig. 10*b*). In contrast to the previous calculations, where $\varphi_s = \varphi_h$, the charges on both boundaries in the present case vary in different ways and one of them even changes sign (see Fig. 10*b*). The disjoining/conjoining isotherm has a maximum in the case (Fig. 10*c*): at high separations repulsion prevails, whereas at small distances attraction is observed.

a)

b)

c)
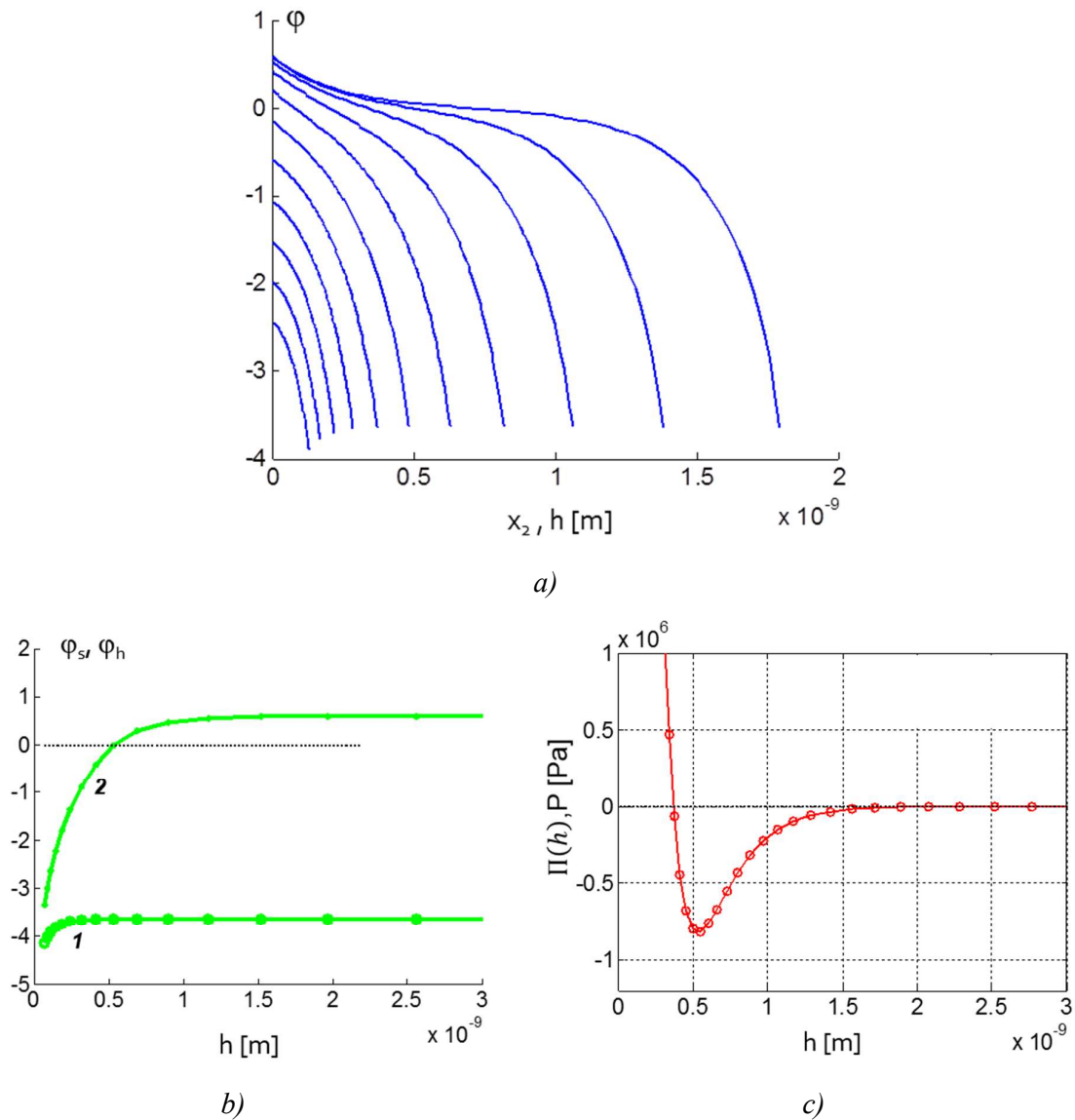
Fig. 11. Interaction of electrically dissimilar surfaces for the case of constant surface charges, $\sigma_{h,s} =$ const: *a*) electric potential distribution, according to Eq. (9): $\sigma_s = -27$ mC, $\sigma_h = 270$ mC; *b*) surface potentials $\varphi_{h,s}$ variation: *1*- liquid/vapour interface, *2*- solid/liquid interface; *c*) disjoining/conjoining pressure isotherm according to Eq. (8).

In Fig. 11 the asymmetric constant charge case is presented: the boundary values of σ are fixed, whereas the boundary electric potentials change and the dependences $\varphi_h(h)$ and $\varphi_s(h)$ do not coincide (see Fig. 11*b*). The disjoining/conjoining pressure isotherm has a minimum in this case (see Fig. 11*c*): an attraction at large separations and a repulsion at small separations.

Let us consider as an example $\varphi_{h,s}$ = constant, which is presented in Fig. 10,*a* in order to understand why the disjoining/conjoining pressure isotherms have a complicated form including the extrema. Since the electric potentials on the boundaries are constant disjoining/conjoining pressure can change only due to a variation of the Maxwell part of disjoining/conjoining pressure (see Eq. (8)).

It is possible to identify three intervals of *h* values corresponding to the different parts of the disjoining/conjoining pressure isotherms (see Fig. 12). In the first interval of low *h* values the gradient $\partial\varphi/\partial x_2$ tends to infinity because for this case $\varphi_{h,s}$ = constant, hence, the difference $\Delta\varphi=\varphi_h$ - φ_s tends to a constant value at $x_2\rightarrow 0$ (Fig. 12, region 1). According to Eq. (8) this implies that $\Pi\rightarrow\infty$ at low separations *h* between the surfaces. In region 2 of the intermediate values of *h,* the gradient $\partial\varphi/\partial x_2$ decreases and at a certain *h* it becomes equal to zero (Fig. 12, region 2). Under these conditions the Maxwell part of disjoining/conjoining pressure is absent and the disjoining/conjoining pressure takes its maximum value which is equal to the excess osmotic pressure in the film according to Eq. (13). Finally, at large distances *h*, the gradient $\partial\varphi/\partial x_2$ becomes negative, reaches its limiting value and does not depend anymore on the increase of *h* (Fig. 12, region 3). In this region the surfaces are non-interacting, and the Maxwell part becomes constant which exactly equals to the excess osmotic pressure, Π_{max}, Eq. (13). This is the reason why the disjoining/conjoining pressure tends to zero at large separations.

The above consideration shows that the maximum of the disjoining/conjoining pressure isotherm is related to the sign change of the gradient $\partial\varphi/\partial x_2$, which is proportional to the surface charge σ (see Eq. (12)): one of the surfaces changes sign of its charge in response to the variation in *h* (see also the calculated σ-dependences in Fig. 10,b). This phenomenon is referred to as a surface charge reversal or overcharging.[18,19] However, the disjoining/conjoining pressure changes its sign not at the point of overcharging, but at the point where the Maxwell part of disjoining/conjoining pressure in Eq. (8) becomes equal to the osmotic part.

A similar analysis can be made for other asymmetric cases. For the condition $\sigma_{h,s}$ = constant shown in Fig. 11 the minimum on the disjoining/conjoining pressure isotherm is explained by the variation of the osmotic part of disjoining/conjoining pressure at the constant Maxwell part. For large values of *h* the electrostatic attraction prevails because the osmotic pressure is weak. At short distances the osmotic pressure in the thin film increases and exceeds the magnitude of the Maxwell term, hence, repulsion is prevailing in this region of thicknesses.
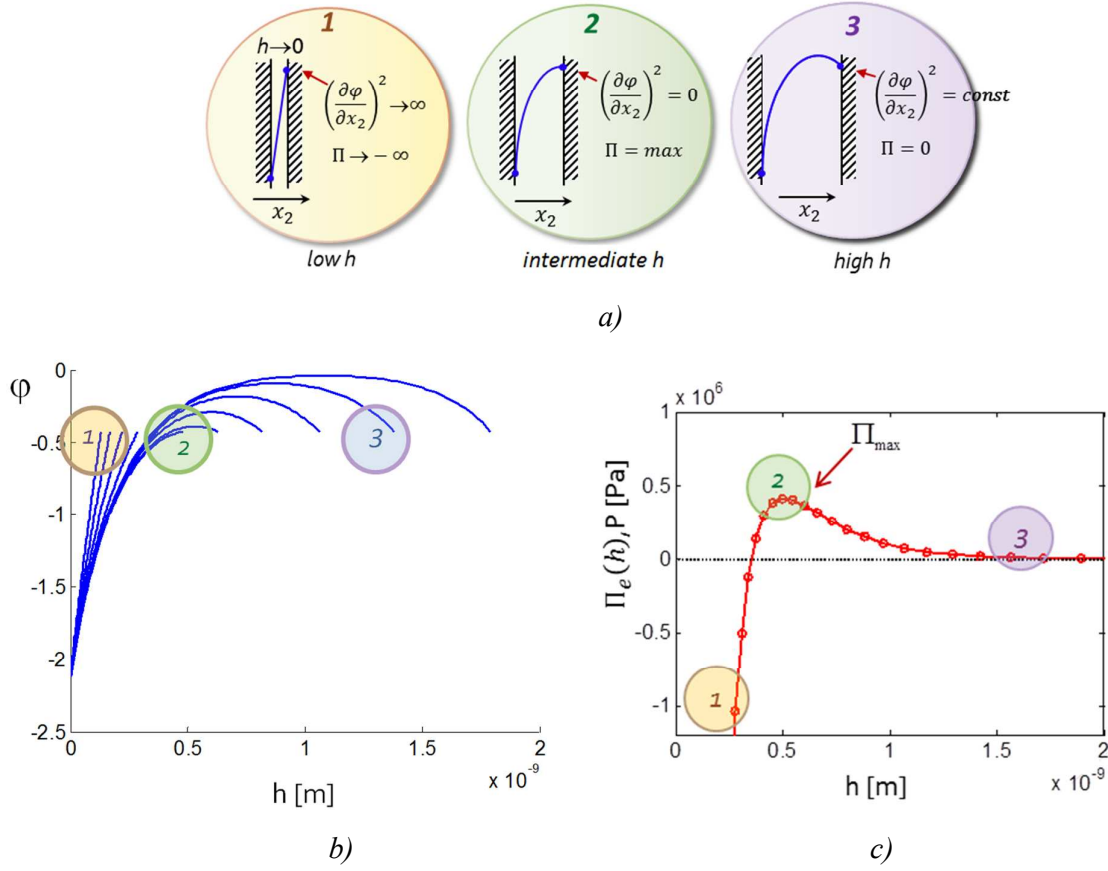
Fig. 12. Analysis of complex character of disjoining/conjoining pressure isotherm for the case $\varphi_{h,s} =$ const; $\varphi_s = -2.12$; $\varphi_h = -0.42$. Three types of electric potential profiles (*a*); the potential distributions at *h* variation (*b*); the calculated disjoining/conjoining pressure isotherm (*c*).

4.4. Equilibrium liquid profile inside the transition zone

Equilibrium liquid profile inside the transition zone is calculated using Eq. (7) obtained from minimising the excess free energy or using Eq. (A14) obtained from the normal stress balance. The radius of the equilibrium meniscus, $r_e = H - h^*$, and the thickness of the equilibrium flat film, h_e are determined by solving the set of Eqs. (11).

The right boundary of the transition zone in x_1-direction was determined from the condition that the calculated profile should be smoothly connected with a spherical part of meniscus. The following parameters were used in the calculations below: $T = 293$ [K]; $c_0 = 1$ [mole/m^3]; $\gamma = 72.7 \times 10^{-3}$ [N/m]; $H = 3 \times 10^{-6}$, [m].

The results of the calculations are presented in Fig. 13. These results confirm that the high values of Π obtained for the highly-charged or high-potential surfaces correspond to thicker flat

equilibrium films (with high capillary pressure). That is, the higher values of the disjoining/conjoining pressure the larger the thickness of the flat equilibrium film, h_e (Fig. 13).

In the case φ = constant the disjoining/conjoining pressure reaches the maximum value Π_{max} at $h \rightarrow 0$ (see the inset in Fig. 13,a). Hence, a critical value of the meniscus radius exists (see Eq. (14)) beyond which equilibrium between the disjoining/conjoining and capillary pressures is no longer possible as discussed above. Thus, equilibrium film thickness h_e cannot increase indefinitely in the case φ = const: a maximum possible value of h_e exists in this case. In contrast, in the σ = constant case the film thickness is not limited by Π_{max} because the disjoining/conjoining pressure increases indefinitely at small h (see the inset in Fig. 13,b).
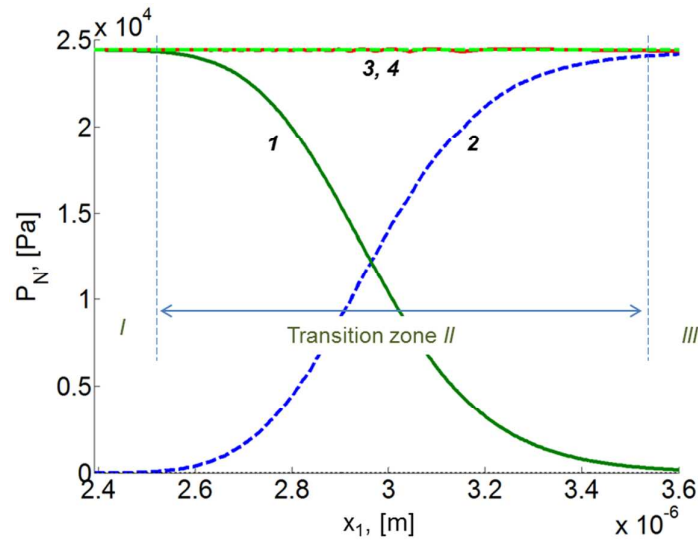
The distribution of the normal stress components in Eq. (7) along x_1 coordinate is given in Fig. 14. The figure illustrates a definition of the transition zone between the flat film and the spherical meniscus as discussed above.

a)

19

b)
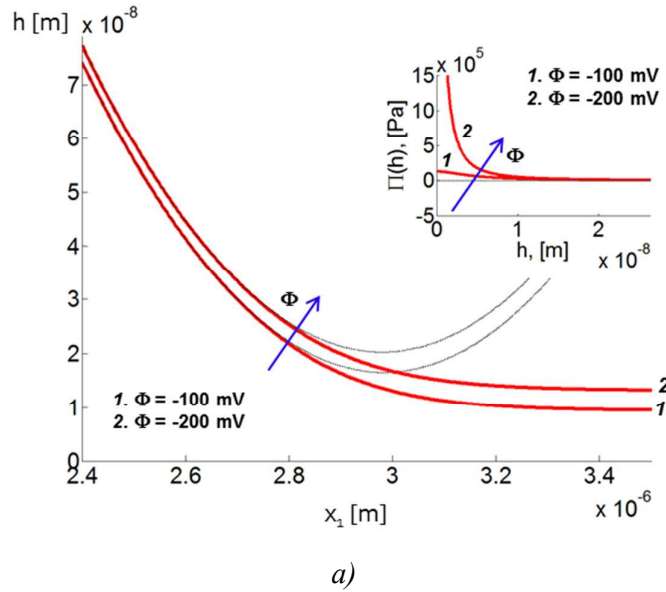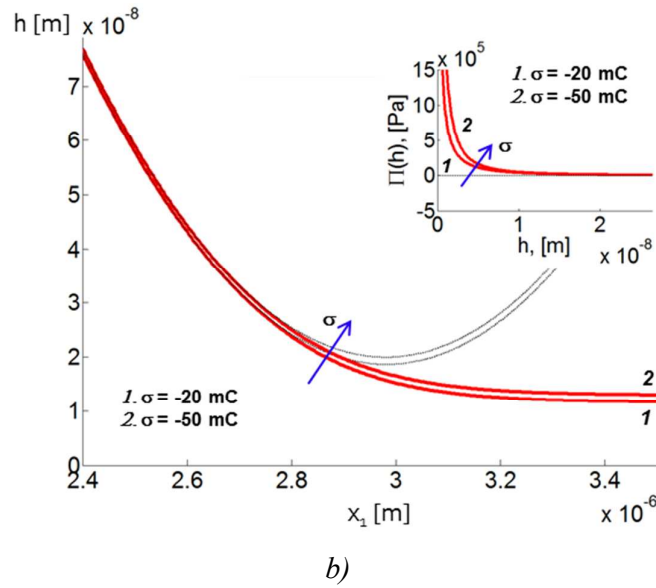
Fig. 13. Equilibrium liquid profiles calculated according to the described above procedure.

(*a*) $\varphi_h = \varphi_s$ = const; (*b*) $\sigma_h = \sigma_s$ = const.

Fig. 14. The normal stress components as functions of x_1 coordinate.

1 – capillary pressure due to the profile curvature, $\gamma h''$; 2 – disjoining/conjoining pressure, Π_e; 3 –
total pressure, $\gamma h'' + \Pi_e$; 4 – excess pressure, P_e, which is capillary pressure for a spherical
meniscus, $\gamma / r_e = \gamma h'' + \Pi_e$.

(I) – zone of a spherical meniscus; (II) – transition zone; (III) – zone of a flat capillary film (see Fig.
3). The complete wetting case: σ_s= -50 mC, σ_h= -50 mC.

4.5. Effect of the van der Waals component

In the previous section only electrostatic component of the disjoining/conjoining pressure was taken into account. The effect of the van der Waals component, Π_W, is calculated as follows[1]:

$$\Pi_W = \frac{A}{6\pi h^3}$$

(15),

where $A = -A_H$ is referred to hereafter as the 'Hamaker constant'; A_H is the original Hamaker constant; h is the separation between the interfaces. The positive (negative) values of the constant A correspond to repulsion (attraction). The following parameters were used in the calculations below: $T = 293$ [K]; $c_0 = 1\times10^3$ [mole/m^3]; $\gamma = 74.7\times10^{-3}$ [N/m]; $H = 3\times10^{-7}$, [m].

For the case of repulsive intermolecular interaction the inclusion of Π_W should increase the disjoining/conjoining pressure and, as a result, lead to a higher thickness of equilibrium film. In Fig. 15 the different types of disjoining/conjoining pressure isotherms and the liquid profiles are presented. The dashed lines correspond to the case when the disjoining/conjoining pressure includes the electrostatic component only, i.e. $\Pi = \Pi_E$. The solid lines correspond to the full DLVO interaction: $\Pi = \Pi_E + \Pi_W$. Lines 1, 2 in Fig. 15 were calculated for a "weaker" electrostatic component ($\Phi_s = \Phi_h$ = -30 mV), lines 3,4 were obtained for a "stronger" electrostatic interaction ($\Phi_s = \Phi_h$ = -150 mV).

In the case of weaker electrostatic interaction (Fig. 15 curve 1), the van der Waals component creates a significant increment in the disjoining/conjoining pressure and the film thickness increases considerably (Fig. 15 curve 2). For the stronger electrostatic interaction (Fig. 15 curve 3), the contribution of the van der Waals component to the disjoining/conjoining pressure is less significant, and only a slight increase in the film thickness is observed (Fig. 15 curve 4).

In Fig. 15 the case of the constant surface potentials, $\varphi_h = \varphi_s$ = constant is presented. For the case $\sigma_h = \sigma_s$ = constant, the effect of Π_W is similar. The van der Waals component leads to an increase in the disjoining/conjoining pressure values and, as consequence, to a growth of the flat film thickness. Additional data on the influence of the disjoining/conjoining pressure components on the liquid profile parameters are shown in Fig. 16.

As in Fig. 15 the dashed lines correspond in Fig. 16 to the case of electrostatic component only, $\Pi = \Pi_E$. The solid lines correspond to the full disjoining/conjoining pressure: $\Pi = \Pi_E + \Pi_W$. Fig. 16 illustrates how the electric properties of the surfaces and van der Waals interaction influence the values of h_e (the equilibrium film thickness) and h^*, where $h^* = H - r_e$) (see Fig. 3).
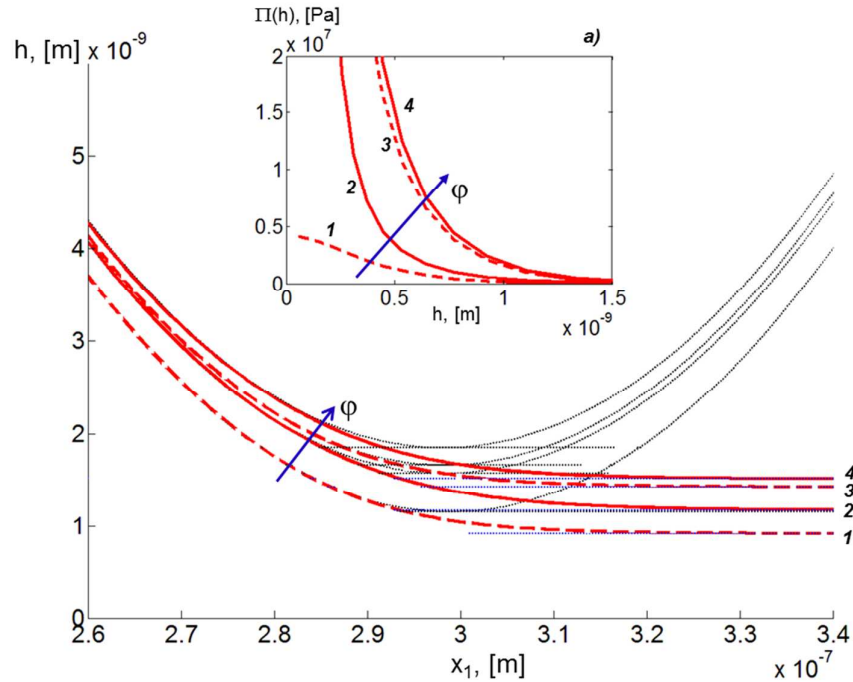
Fig. 15. Influence of van der Waals component of disjoining/conjoining pressure on the liquid profile for the case $\varphi_h = \varphi_s = $ const. The thick dashed lines: a single electrostatic component of disjoining/conjoining pressure; the solid lines: electrostatic + van der Waals components of disjoining/conjoining pressure (Hamaker constant $A = 5\times10^{-21}$ J). 1. $\Phi_{s,h} = $ -30 mV, $\Pi = \Pi_E$; 2. $\Phi_{s,h} = $ -30 mV, $\Pi = \Pi_E + \Pi_W$; 3. $\Phi_{s,h} = $ -150 mV, $\Pi = \Pi_E$; 4. $\Phi_{s,h} = $ -150 mV, $\Pi = \Pi_E + \Pi_W$.

For the case of constant surface potentials, $\varphi_h = \varphi_s = $ const (Fig. 16,*a*), the higher the absolute value of electric potential the bigger the values h_e and h^*. In the case of full disjoining/conjoining pressure (solid lines), the disjoining/conjoining pressure is higher due to van der Waals interaction and there is an increase in h_e and h^* values in comparison with a case of a single electrostatic component (dashed lines). As also shown in Fig. 16,*a* the biggest difference between the cases Π_E and $\Pi_E + \Pi_W$ is observed at Φ values close to zero (curves 1,2 vs. 3,4 in Fig.16,*a*): the influence of the van der Waals component is the most pronounced at a low electrostatic interaction. The effect of the van der Waals interaction on h_e and h^* reduces while increasing the electrostatic part of disjoining/conjoining pressure.

22
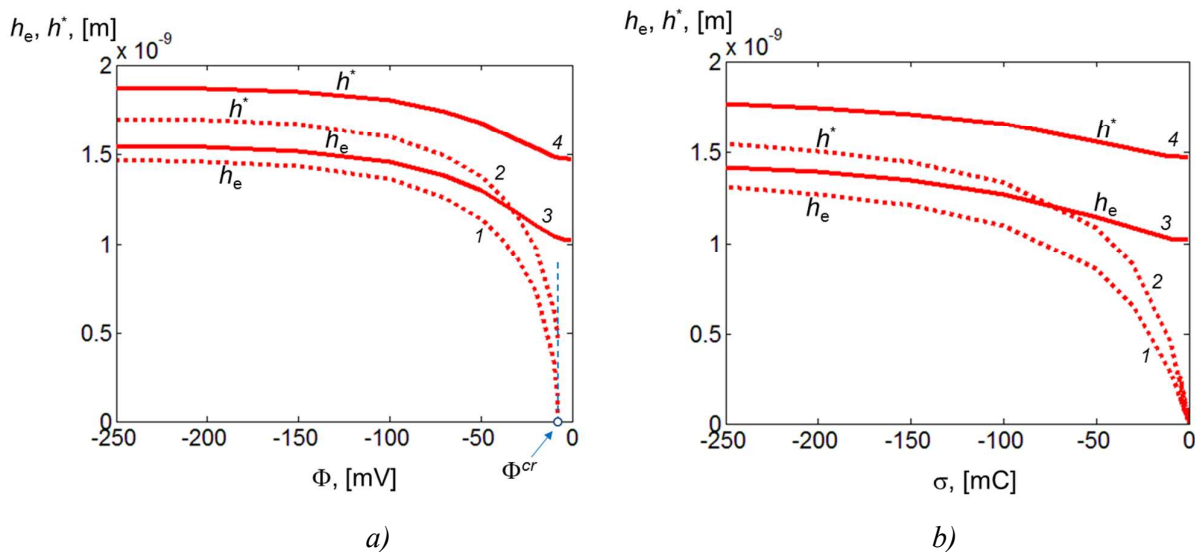
Fig. 16. Dependence of h_e and h^* on the surface values of electric potentials (a) and the surface charge densities (b).

a) constant surface potentials, $\varphi_h = \varphi_s = const$; b) constant surface charges, $\sigma_h = \sigma_s = const$.

1,2 - electrostatic component only, $\Pi = \Pi_E$; 3,4 - sum of electrostatic and van der Waals components, $\Pi = \Pi_E + \Pi_W$ ($A = 5 \times 10^{-21}$ J).

1,3 - equilibrium film thickness h_e; 2,4 - $h^* = H - r_e$.

When the electrostatic component is the only one contributing to disjoining/conjoining pressure (curves 1,2 in Fig. 16,a) the curves h_e and h^* do not tend to zero at $\Phi \rightarrow 0$. The zero value of h_e corresponds to a certain critical value of electric potential Φ^{cr} (Fig. 16,a), because the meniscus cannot exist at very low electric potentials, when $\Phi < \Phi^{cr}$. The critical value of Φ is related to a magnitude Π_{max} (see Eq. (13)) beyond which equilibrium between disjoining/conjoining and capillary pressures is impossible. The value of Π_{max} decreases with Φ decrease, and at value Φ^{cr} the magnitude Π_{max} becomes too low to counterbalance the existing value of capillary pressure. Thus, a critical electric potential Φ^{cr} is a parameter similar to a critical capillary width H^{cr}, which was introduced earlier (Eq. (14)). These both parameters follow from the condition of the equilibrium between capillary and disjoining/conjoining pressures (see section 4.2). For the case presented in Fig. 16,a, the critical value $\Phi^{cr} = - 7.8$ mV.

For the case of full DLVO interaction, $\Pi = \Pi_E + \Pi_W$ (solid lines in Figs.16,a,b) the magnitudes h_e and h^* tend to non-zero values at $\Phi \rightarrow 0$ (Fig.16,a) or $\sigma \rightarrow 0$ (Fig.16,b). These non-zero values of h_e and h^* are the same for both cases and correspond to conditions when the van der Waals interaction included only, i.e. $\Pi = \Pi_W$, $\Pi_E = 0$.

23

If disjoining/conjoining pressure includes the electrostatic component only (dashed lines for the case $\sigma_h = \sigma_s = $ const (Fig.16,*b*)) then the dependencies h_e and h^* tend to zero at $\sigma \to 0$ (in contrast to situation in Fig.16,*a*): equilibrium between disjoining/conjoining and capillary pressures is possible at very small thicknesses h in the case $\sigma_h = \sigma_s = $ const (see Fig. 8). Fig.16,*b* shows also that the difference $h^* - h_e$ decreases at $\sigma \to 0$ (lines 1,2). That means the shrinking of the transition zone between a spherical meniscus and a flat wetting film in the case of constant surface charges.

4.6. Equilibrium liquid profile under partial wetting conditions

The previous consideration was carried out for the case of complete wetting conditions. To calculate the liquid profile for the partial wetting case it is necessary to use the disjoining/conjoining pressure isotherm which includes the attractive interaction (negative values of disjoining/conjoining pressure) and gives the values $\cos \theta_e < 1$ calculated according to Eq. (2).

For the case of partial wetting the continuation of the spherical meniscus intersects the flat liquid film at a contact angle θ_e (Fig. 17). Since the values of θ_e could be high the condition $h' \ll 1$ used above could not be always satisfied for the case of partial wetting conditions. The set of Eqs. (11) deduced for the case of complete wetting is not applicable anymore for the calculation of the film thickness h_e and the meniscus radius r_e.
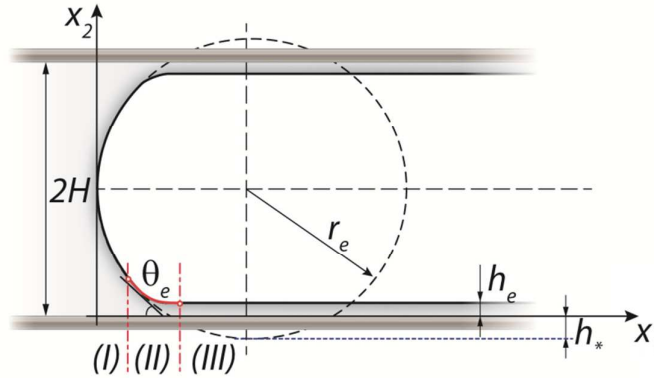
Fig. 17. Meniscus in the case of partial wetting.

In this case $r_e > H$, so $h^* = H - r_e < 0$.

In this case it is more convenient to solve directly Eq. (6). Integration of this equation using boundary condition $h'(h \to H) = -\infty$ results in the following first-order differential equation:

$$\frac{dh}{dx_1} = -\sqrt{-1 + \frac{\gamma^2}{\left[\frac{\gamma}{r_e}(H-h) - \int_h^\infty \Pi_e dh\right]^2}}$$ (16)

Solution of Eq. (16) should satisfy the boundary conditions in the region of a flat film:

$$h(\infty) = h_e; \ h'(\infty) = 0.$$

Substitution of $h = h_e$ and $h' = 0$ into Eq. (16) and using $r_e = H - h^*$ gives a relation between h^* and h_e:

$$h^* = H - \frac{H - h_e}{1 + \frac{1}{\gamma} \int_{h_e}^{\infty} \Pi_e dh} \tag{17}$$

Thus, the values h^* and h_e are found by solving Eq. (17) in combination with the first equation from the system (11). After this the liquid profile in the transition zone is calculated according to Eq. (16).

An example of the calculation for the partial wetting case in comparison with the complete wetting conditions is given in Fig. 18. This figure shows that the transition between the flat film and the spherical meniscus is sharter in the case of partial wetting (curve 2 in Fig. 18). This behaviour is caused by the attractive part of the isotherm for the case of partial wetting conditions (see inset in Fig. 18).

A distribution of the normal stress components in x_1 direction (Fig. 19) shows that disjoining/conjoining pressure (curve 2) is positive in the zone III of a flat film, then it changes its sign in the transition zone II (becomes negative with h increase, according to the isotherm form). At high h in the region III of spherical meniscus, disjoining/conjoining pressure tends to zero. The value of local capillary pressure $\gamma K = \gamma h'' / (1 + h'^2)^{3/2}$ (curve 1) changes oppositely to disjoining/conjoining pressure so that a total pressure (a sum of disjoining/conjoining and capillary pressures, curve 3) remains constant along x_1 axis (Fig. 19).

The values of a local capillary pressure directly determine a shape of the liquid profile. Capillary pressure takes the maximum value under the complete wetting conditions in the region of a spherical meniscus (Fig. 14, curve 1), i.e. the liquid profile has the maximum curvature in this area. In the partial wetting case capillary pressure reaches the maximum inside the transition zone (Fig. 19, curve 1), so the liquid profile has the maximum curvature here (Fig. 18, curve 2).
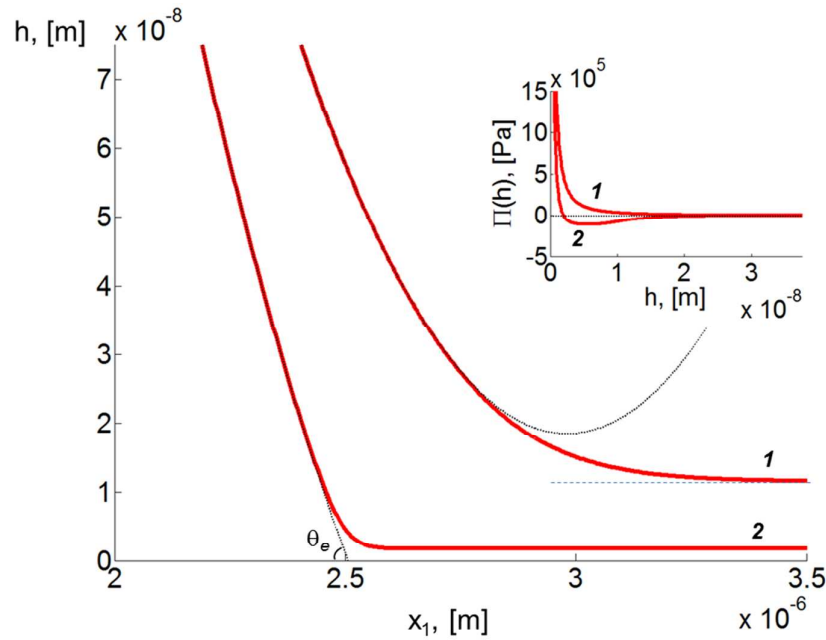
Fig. 18. Comparison of the liquid profiles for the cases of complete and partial wetting.
1. complete wetting (θ_e=0): σ_s= -100 mC, σ_h= -10 mC, $\Pi_W = 0$; 2. partial wetting (θ_e=10.4°): σ_s= -100 mC, σ_h= 10 mC, $\Pi_W = 0$; $c_0 = 1$ mole m^{-3}.

The partial wetting case presented in Figs. 18 and 19 is characterized by the value of the equilibrium contact angle θ_e=10.4°. This value was calculated using Eq. (2) at $h_e = 1.85 \times 10^{-9}$ m. It should be noted that only one of the possible types of the equilibrium liquid profile under the partial wetting conditions is presented in Fig. 18. Other forms of the transitional profiles and other values of θ_e can be found by variation of the disjoining/conjoining pressure isotherm.

The character and intensity of the surface forces have a decisive effect on the liquid profile inside the transition zone. In general a growth of a flat film thickness is observed with an increase of the disjoining/conjoining pressure values due to augmentation of the electrostatic or van der Waals components.
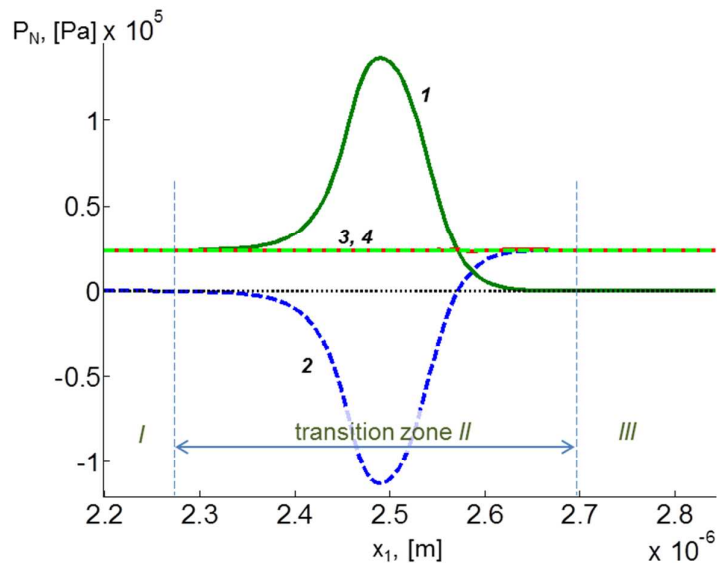
Fig. 19. The normal stress components as functions of x_1 coordinate for the case of partial wetting. 1 – capillary pressure due to the profile curvature, γK; 2 – disjoining/conjoining pressure, Π_e; 3 – total pressure, $\gamma K + \Pi_e$; 4 – excess pressure, $P_e = \gamma / r_e = \gamma K + \Pi_e$. (I) – zone of a spherical meniscus; (II) – transition zone; (III) – zone of a flat capillary film (see Fig. 3). The partial wetting case ($\theta_e > 0$): $\sigma_s = -100$ mC, $\sigma_h = 10$ mC, $\Pi_W = 0$, $\theta_e = 10.4°$.

5. Conclusion

Inside a transition zone between the spherical part of a meniscus and a thin wetting film in front the combined action of capillary and disjoining/conjoining pressures determines the liquid shape. The model was developed for both complete and partial wetting cases. The low-slope approximation for the liquid profile inside the transition zone was used. Expression for the electrostatic component of disjoining/conjoining pressure was derived. The equilibrium meniscus radius and film thickness were obtained using a method of matching of the inner and outer asymptotic solutions. Both cases of complete and partial wetting are considered.

The presented theory allows calculating equilibrium liquid profile inside the transition zone, equilibrium contact angles, the disjoining/conjoining pressure isotherms, and the distribution of electric field inside the liquid phase. The electrostatic parts of the disjoining/conjoining pressure isotherms were calculated by solving the Poisson-Boltzmann equations. The cases of different boundary conditions for electric potential distribution at liquid/vapour and liquid/solid interfaces were considered and compared.

In the case of the interacting surfaces with similar charges or potentials the electrostatic component of disjoining/conjoining pressure, $\Pi(h)$, is a monotonous function (completely increasing or decreasing). In the case of dissimilar interacting surfaces the dependency $\Pi(h)$ can include maximum or minimum. This complicated form of disjoining/conjoining pressure isotherms is explained by the fact that the osmotic and Maxwell parts of the electrostatic interaction changes in different way in response to the variation of h. As a result the difference between them (equal to $\Pi(h)$) can change its sign and include the extrema.

Our results prove that the form of the disjoining/conjoining pressure isotherm has a decisive effect on the shape of the equilibrium interfacial profile inside the transition zone: the higher disjoining/conjoining pressure, the larger the thickness of the equilibrium flat film and the lower value of the radius of equilibrium meniscus. For the partial wetting case isotherms have a negative (i.e. attractive) part on the interaction curve: the deeper the attraction minimum the thinner the equilibrium flat film and the higher the contact angle value. The sharper form of the profile within the transition zone for partial wetting case is related to the attraction minimum: the stronger the attraction the sharper the transition between the flat film and spherical part of the meniscus. The inclusion of the van der Waals component in the disjoining/conjoining pressure leads to its increase, and, as a result, a growth of the flat film thickness and a decrease of the meniscus radius.

A critical width of capillary is introduced for characterisation of the possibility of the flat film existence in thin capillaries: at small H the capillary pressure is high and cannot be counterbalanced by the electrostatic component of disjoining/conjoining pressure which has the limiting maximum value Π_{max} for the case of constant surface electric potentials. For the flat films under these conditions the mechanical equilibrium is impossible, the equilibrium thickness, h_e, of the films tends to zero. Similarly, the critical value of the surface electric potential is introduced: for the potential values below the critical one the electrostatic interaction is too weak and the disjoining/conjoining pressure cannot counterbalance the existing value of capillary pressure. There is a 'prohibited' zone characterized by low values of the surface potential and small values of the capillary width H, where the equilibrium between capillary and disjoining/conjoining pressures is not achieved.

Appendix 1

Expression for electrostatic component of disjoining/conjoining pressure

The electric field distribution inside the liquid is described by the Poisson equation:

$$\varepsilon\varepsilon_0\left(\frac{\partial^2\Phi}{\partial x_1^2}+\frac{\partial^2\Phi}{\partial x_2^2}\right)=-q\,,\tag{A1}$$

where q is electric charge density, which is a function of the ion concentrations:

$$q = F[c_+(x_1,x_2)-c_-(x_1,x_2)].$$

The flux of ions $J_\pm = -D_\pm\nabla c_\pm \mp F/(RT)\,D_\pm c_\pm\nabla\Phi$ vanishes at equilibrium in any direction, where $D_\pm$ are diffusion coefficients.

Let us introduce a dimensionless electric potential as $\varphi = \dfrac{F\Phi}{RT}$. Then, the equation for ion flux becomes $\vec{J}_\pm = -D_\pm\nabla c_\pm \mp D_\pm c_\pm\nabla\varphi$. Hence, from the equilibrium conditions, we have:

$$0 = -\frac{\partial c_\pm}{\partial x_1}\mp c_\pm\frac{\partial\varphi}{\partial x_1}$$

$$0 = -\frac{\partial c_\pm}{\partial x_2}\mp c_\pm\frac{\partial\varphi}{\partial x_2}$$

Integration of the latter two equations results in

$$c_\pm(x_1,x_2) = A_{\pm 1}(x_2)\exp(\mp\varphi)$$

$$c_\pm(x_1,x_2) = A_{\pm 2}(x_1)\exp(\mp\varphi)\tag{A2}$$

where $A_{\pm 1}(x_2),\quad A_{\pm 2}(x_1)$ are integration functions. Comparison of the latter two equations shows that $A_{\pm 1}(x_2)=A_{\pm 2}(x_1)=const=a_\pm$. In the bulk solution, where the electric potential is equal to zero, electroneutrality is satisfied, hence, $a_+=a_-=c_0$, where c_0 is concentration of anions and cations in the bulk solution. That is, the concentrations from Eq. (A2) can be rewritten as

$$c_\pm(x_1,x_2) = c_0\exp(\mp\varphi)\tag{A3}$$

Substitution of Eq. (A3) into Eq. (A1) results in the well- known Poisson-Boltzmann equation for the electrical potential:

$$\left(\frac{\partial^2\varphi}{\partial x_1^2}+\frac{\partial^2\varphi}{\partial x_2^2}\right)=\frac{F^2c_0}{\varepsilon\varepsilon_0 RT}\left(\exp(\varphi)-\exp(-\varphi)\right)\tag{A4}$$

According to the low-slope assumption we can neglect variations with respect to x_1 inside the transition zone ($\partial\ /\partial x_1 \ll \partial\ /\partial x_2$):

$$\frac{\partial^2 \varphi}{\partial x_2^2} = \frac{F^2 c_0}{\varepsilon\varepsilon_0 RT}\left(\exp(\varphi) - \exp(-\varphi)\right) \tag{A5}$$

In the case of equilibrium, the momentum equations in the x_1 and x_2 directions are expressed as follows[14,15]:

$$-\frac{\partial p}{\partial x_1} - q\frac{RT}{F}\frac{\partial \varphi}{\partial x_1} = 0, \tag{A6}$$

$$-\frac{\partial p}{\partial x_2} - q\frac{RT}{F}\frac{\partial \varphi}{\partial x_2} = 0. \tag{A7}$$

Substitution $q = Fc_0\left(\exp(-\varphi) - \exp(\varphi)\right)$ into the latter two equations results in

$$\frac{\partial}{\partial x_1}\left[p - RTc_0\left(\exp(\varphi) + \exp(-\varphi)\right)\right] = 0.$$

$$\frac{\partial}{\partial x_2}\left[p - RTc_0\left(\exp(\varphi) + \exp(-\varphi)\right)\right] = 0.$$

Integration of these equations yields

$$p - RTc_0\left(\exp(\varphi) + \exp(-\varphi)\right) = C_1 \tag{A8}$$

where C_1 is an integration constant. Eq. (A8) shows that the sum of the hydrostatic and osmotic pressures remains constant throughout the whole system.

The excess pressure P_e in Kelvin's equation given by Eq. (1) is equal to the capillary pressure in the region of the spherical meniscus (region I in Fig 3):

$$\frac{RT}{v_m}\ln\frac{p_s}{p_e} = \frac{\gamma}{r_e}, \tag{A9}$$

The normal stress balance for a liquid film in the transition zone[3] is:

$$-p + -\frac{1}{2}\varepsilon\varepsilon_0 E^2 + \varepsilon\varepsilon_0 E_2^2 = \frac{d}{dx_1}\frac{\gamma h'}{\sqrt{1+h'^2}}, \quad x_2 = h \tag{A10}$$

where $E_i = -\frac{RT}{F}\frac{\partial \varphi}{\partial x_i}$ is the electric field.

Taking into account that $\partial\ /\partial x_1 \ll \partial\ /\partial x_2$, Eq. (A10) can be written as:

$$-p\big|_{x_2=h} + \frac{(RT)^2\varepsilon\varepsilon_0}{2F^2}\left(\frac{\partial \varphi}{\partial x_2}\right)^2_{x_2=h} = \gamma h'' \tag{A11}$$

Combination of Eqs. (A11) and (A8) results in:

$$\gamma h'' + \Pi(h) = C_1 - 2RTc_0 \tag{A12},$$

30

where

$$\Pi(h) = RTc_0\big(\exp(\varphi) + \exp(-\varphi)\big)\Big|_{x_2=h} - \frac{(RT)^2 \varepsilon\varepsilon_0}{2F^2}\left(\frac{\partial\varphi}{\partial x_2}\right)^2_{x_2=h} - 2RTc_0 \tag{A13}$$

is the normal component of disjoining/conjoining pressure, Π, which coincides with the well-known expression for the electrostatic part of the disjoining/conjoining pressure.[1,16] According to Eq. (A13) at high separations $\Pi(h \to \infty) = 0$ and $\varphi(h \to \infty) = 0$. These conditions mean that the electric field and disjoining/conjoining pressure vanish at large distance between the surfaces.

It is easy to check that the disjoining/conjoining pressure is constant in the normal direction by differentiating Eq. (A13) with respect to x_2 :

$$\frac{d\Pi}{dx_2} = \left[RTc_0\big(\exp(\varphi) + \exp(-\varphi)\big) - \varepsilon\varepsilon_0\left(\frac{RT}{F}\right)^2 \frac{\partial^2\varphi}{\partial x_2^2}\right]\frac{\partial\varphi}{\partial x_2} = 0 .$$

Since the terms in the bracket correspond to the Poisson-Boltzmann equation, it follows that the disjoining/conjoining pressure remains constant in the normal direction not only in the case of flat films,[5,9] but also in the case of low-slope films. Hence, to write down a normal stress balance, any x_2 plane can be chosen. In the above expressions a value $x_2=h$ corresponding to a vapour/liquid interface was selected. The constant in Eq. (A12) becomes $C_1 - 2RTc_0 = \dfrac{\gamma}{r_e}$ and $C_1 = \dfrac{\gamma}{r_e} + 2RTc_0$.

Hence, the equation for the liquid profile is

$$\gamma h'' + \Pi_e(h) = \frac{\gamma}{r_e} , \tag{A14}$$

and $p = RTc_0\big(\exp(\varphi) + \exp(-\varphi) - 2\big) + \dfrac{\gamma}{r_e}$.

Equation (A14) has been obtained using the condition of normal stress balance, Eq. (A10). The obtained equation coincides with Eq. (7) which was derived from the principle of the excess free energy minimisation (4). Thus, the same equation is obtained in this section using completely different approach.

Appendix 2

The matching inner and outer solutions

The equilibrium film thickness h_e and the meniscus radius r_e (see Fig. 3) are determined by matching the inner and outer asymptotic solutions. In region *I* where electrical double layers do not overlap, the liquid profile is described as follows:

$$\frac{\gamma h''}{\left[1+\left(h'\right)^2\right]^{3/2}} = P_e = \frac{\gamma}{H-h_*},$$

where $r_e = H - h*$ (see Fig 3).

Integration of the latter equation with boundary condition $h(0)=H$ results in the following solution for the spherical meniscus:

$$h(x_1) = H - \sqrt{\left(H-h_*\right)^2 - \left(x_1 - \left(H-h_*\right)\right)^2} \qquad (A15)$$

Introducing the dimensionless variables: $\xi = h/h_e$, and $y = [x_1-(H-h_*)]/l$, where l is a length scale along x_1, $l = \sqrt{h_e\left(H-h_*\right)}$, which is the length scale of the transition zone. Using these variables Eq. (A15) can be rewritten close to the position of the minimum film thickness in Fig. 3:

$$\xi(y) = \frac{h*}{h_e} + \frac{y^2}{2} . \qquad (A16)$$

The unknown value $\dfrac{h*}{h_e}$ can be determined by matching the solution according to (A16) and inner solution, Eq. (A14), at y→-∞.

Let us introduce the same dimensionless variables ξ and y in Eq. (A14):

$$\frac{d^2\xi}{dy^2} + f(\xi) = 1, \quad \xi(\infty) = 1,$$

where $f(\xi) = \dfrac{H-h*}{\gamma}\Pi_e(h)$. Let us introduce a new unknown function in the latter equations:

$p(\xi) = \xi'$; then, $p(\xi)p'(\xi) = 1 - f(\xi)$, $p(1) = 0$. After integration

$$\xi' = -\sqrt{2\left(\xi - 1 - \int_1^\xi f(\xi)d\xi\right)}$$

From the latter equation at $y \rightarrow -\infty$:

$$\xi' = -\sqrt{2\xi - 2\left(1 + \int_1^\infty f(\xi)d\xi\right)}$$

Eq. (A16) can be also rewritten as:

$$\xi' = -\sqrt{2\xi - \frac{2h*}{h_e}}$$

Comparison of the two latter equations results in:

$$h^* = h_e\left(1 + \int_1^\infty f(\xi)d\xi\right).$$

Hence, the following relation between h_e and h^* should be satisfied for matching of the inner and outer solutions:

$$h_* = h_e + \frac{H - h^*}{\gamma}\int_{h_e}^\infty \Pi_e(h)dh$$

(A17)

References
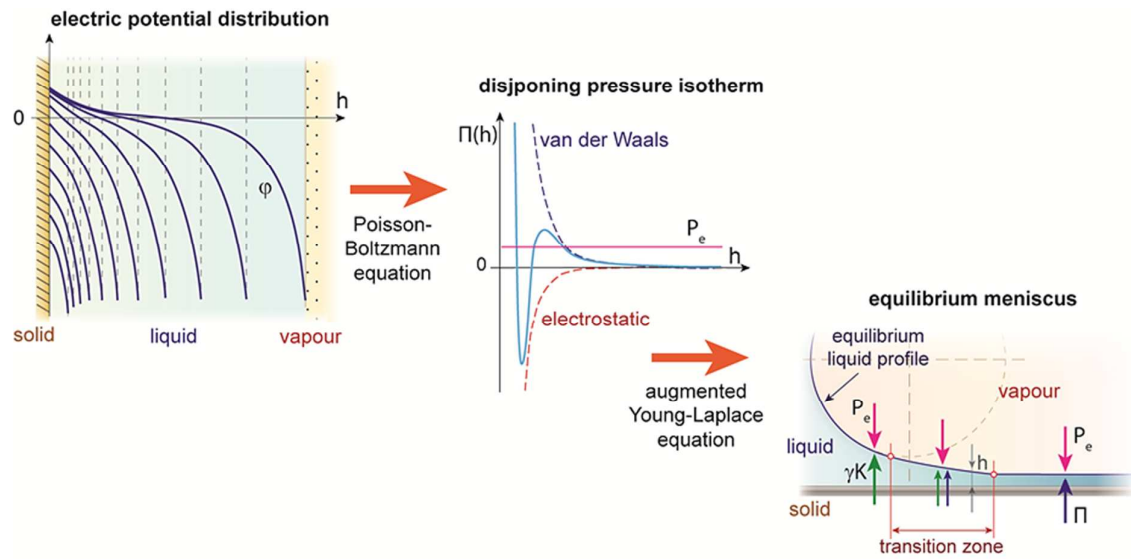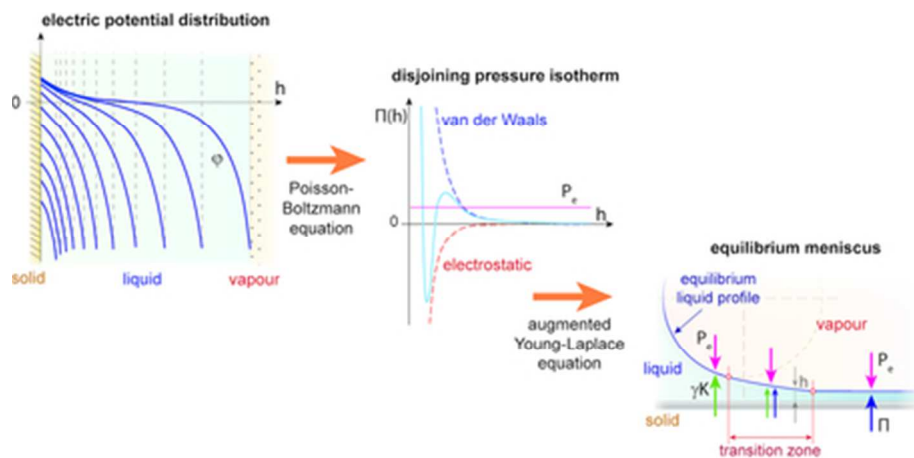
1. B.V. Derjaguin, N.V. Churaev, V.M. Muller. *Surface Forces*. Springer, 1987.

2. B.V. Derjaguin. *Colloid J.*, 1955, **17**(3), 191–197.

3. V.M. Starov, M.G. Velarde, C.J. Radke. *Wetting and Spreading Dynamics.* New York: Taylor and Francis/CRC, 2007.

4. N.V. Churaev, V.D. Sobolev. *Adv in Colloid and Int Sci*, 1995, **61**, 1–16.

5. P.A. Kralchevsky, I.B. Ivanov. *Chem. Phys. Lett.*, 1985, **121**, 111–115.

6. I.B. Ivanov, B.V. Toshev. *Colloid Polym. Sci.*, 1975, **253**, 593–599.

7. N.V. Churaev, V.M. Starov, B.V. Derjaguin. *J Colloid Interface Sci.*, 1982, **89**(1), 16–24.

8. B.V. Derjaguin, N.V. Churaev. *J Colloid Interface Sci.*, 1976, **54**(2), 157–175.

9. B.V. Derjaguin, N.V. Churaev. *J Colloid Interface Sci.*, 1978, **66**(3), 389–398.

10. V.M. Starov, M.G. Velarde. *J. Phys.: Condens. Matter*, 2009, **21**, 464121.

11. P.G. de Gennes. *Rev. Mod. Phys.* 1985, **57** (3), 827–863.

12. R. V. Craster, O. K. Matar. *Rev. Mod. Phys.*, 2009, **81**(3), 1131–1198.

13. G. Karapetsas, R. V. Craster, O. K. Matar. *J. Fluid Mech.*, 2011, **670**, 5–37.

14. A.I. Zhakin. Electrohydrodynamics. *Physic -Uspekhi*, 2012, **55**(5), 465–488.

15. *Electrohydrodynamics*. Edited by A. Castellanos. Springer, 1998.

16. H.J. Butt, K. Graf, M. Kappl. *Physics and Chemistry of Interfaces*. WILEY-VCH Verlag, 2003.

17. O. Stern. *Z. Elektrochem.*, 1924, **30**, 508–516.

18. J. Lyklema. *Colloids Surf. A*, 2006, **291**, 3–12.

19. A. Martin-Molina, C. Rodriguez-Beas, R. Hidalgo-Alvarez, M. Quesada-Perez. *J. Phys. Chem. B*, 2009, **113**, 6834–6839.

20. J.S. Rowlinson, B. Widom. *Molecular Theory of Capillarity*. Clarendon Press, 1982.

21. J.R. Henderson. *PRE* **72**, 051602 (2005).

22. J.R. Henderson. *Eur.Phys.J.Spec.Topics* **197**, 115 (2011).

electric potential distribution

0

φ

solid   liquid   vapour

Poisson-
Boltzmann
equation

disjponing pressure isotherm

Π(h)   van der Waals

P_e

0   h

electrostatic

augmented
Young-Laplace
equation

equilibrium meniscus

equilibrium
liquid profile

vapour

P_e

liquid P_e

γK h P_e

solid   Π

transition zone

38x18mm (300 x 300 DPI)